ISSN : 0974 - 7486 Volume 7 Issue 1

Trade Science Inc.

Materials Science

An Indian Journal

Full Paper

MSAIJ, 7(1), 2011 [59-65]

As-cast microstructures of {M-30Cr-0 to 5% C} ternary alloys.

Part II: Cobalt-base alloys

Patrice Berthod[1,2]*, Ophelie Hestin[1], Elise Souaillat[1]

[1]Faculty of Sciences and Technologies, B.P. 70239, 54506 Vandoeuvre-lès-Nancy, (FRANCE)

[2]Institut Jean Lamour (UMR 7198), Department of Chemistry and Physics of Solids and Surfaces,
B.P. 70239, 54506 Vandoeuvre-les-Nancy, (FRANCE)

E-mail : Patrice.Berthod@lcsm.uhp-nancy.fr

Received: 3rd September, 2010 ; Accepted: 13th September, 2010

ABSTRACT

As seen before with nickel alloys, high carbides fractions can be easily obtained in cast alloys, simply by choosing sufficiently high carbon contents in presence of chromium. This allows obtaining alloys, potentially able to offer very high values of hardness. To quantify the carbides fractions which can be possibly obtained, cobalt alloys containing high contents in carbon and chromium were the subject of a preliminary study by thermodynamic calculations. Thereafter thirteen 30wt.%Cr-containing Co-based alloys with an increasing carbon content (from 0 to 5wt.%) were really elaborated by foundry and their microstructures were characterized by electron microscopy and image analysis. The alloys with less than 3-3.5wt.%C display a hypoeutectic microstructure composed of matrix dendrites and eutectic carbides. For higher carbon contents dendrites are replaced by coarse primary carbides. Graphite may also appear, but only for very high carbon contents (5wt.% C) which allows obtaining carbides fractions greater than for nickel alloys.

KEYWORDS

Cobalt alloys;
High chromium;
Very high carbon;
Thermodynamic calculations;
Solidification;
Microstructure.

INTRODUCTION

Cobalt-based alloys rich in chromium are used in numerous fields, and as already evocated in the first article which dealt with nickel alloys[1], one can cite some alloys for prosthetic dentistry[2], hot parts in aeronautic and power generation turbine disks[3] as well as other applications like some of the fiberizing tools used in the glass industry[4]. Generally several tens weight percent of chromium are effectively added to cobalt to allow the alloy sufficiently resisting wet or atmospheric corrosion, hot corrosion by various molten substances (salts, glasses), as well as high temperature oxidation. In these applications, the intrinsic hardness of such alloys often represents a problem since their base element (cobalt) is a hard metal and thus it promotes high hardness values for the alloys, generally higher than for nickel or iron-based alloys. This can result in more severe difficulties when the pieces must be machined after the foundry process. In contrast, such great hardness is welcome in other practical applications of cobalt alloys, for example for cutting tools[5] made of a cobalt matrix

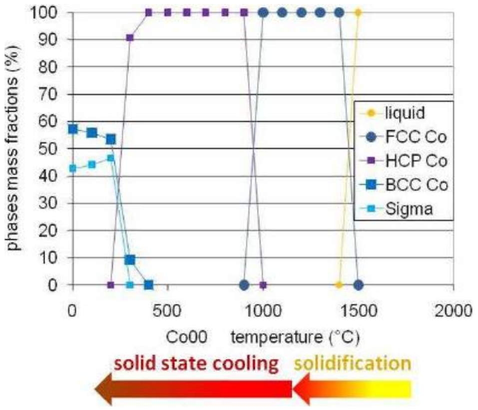

Figure 1 : Stable metallurgical states of the Co00 alloy as calculated by Thermo-Cal; qualitative illustration of the microstructure development during the solidification progress

containing high amounts of dispersed WC carbides, or for coatings[6] consisting in Co-W$_2$C deposited by thermal spray on steels.

As for the nickel alloys studied in the first part of this work[1], great quantities of carbon can be added in {Co, Cr}-based alloys in order to obtain very high values of hardness thanks to the carbides intrinsic hardness (much more than 1000 Hv)[7], since the hardness of the whole alloy is logically attended to increase with the carbides volume fraction in the cobalt-based alloys too[8]. Knowing the carbides quantities which can be achieved by increasing the mass of carbon added to the alloy in presence of chromium playing the role of carbide-former element, one can imagine the potential of hardening that such metallurgical system is capable to offer.

Here, a wide variety of cobalt-based alloys containing the same chromium quantity and a carbon content varying in the same range as for the nickel alloys of the first part of this work[1], following a preliminary theoretical study of the solidification and of the solid state cooling sequences by thermodynamic calculations destined to prospect the microstructures which can be expected, were really elaborated by foundry and characterized by metallography.

EXPERIMENTAL

Initial thermodynamic calculations

Preliminary to their real elaborations, thermodynamic calculations were performed to anticipate the characteristics of the microstructures which may appear, in terms of type and quantities of the solid phases (carbides, intermetallic phases, even graphite when the carbon contents are very high). The N-version of the Thermo-Calc software[9], working with a database containing the descriptions of the Co-Cr-C systems and its sub-systems[10-15], was used for this exploration. The thermodynamically stable microstructures were thus calculated for all the temperatures between 1500°C and 0°C, step 100°C. Here too, the theoretic microstructure characteristics are of course not realist for temperatures under 400°C (and even more), for kinetic reasons.

Elaboration and metallographic characterization of the alloys

As for the nickel alloys of the first part of this work, the thirteen Co-30wt.%Cr-xC alloys which were considered here have a targeted carbon content equal to 0 (alloy named “Co00”), 0.2 (Co02), 0.4 (Co04), 0.8 (Co08), 1.2 (Co12), 1.6 (Co16), 2.0 (Co20), 2.5 (Co25), 3.0 (Co30), 3.5 (Co35), 4.0 (Co40), 4.5 (Co45) and 5.0 wt.%C (Co50). They were elaborated by foundry from pure elements (cobalt and chromium: Alfa Aesar, purity higher than 99.9 wt.%; carbon: graphite), which were melted together under an inert atmosphere generated with Argon U (300millibars), and an ingot of several tens grams was obtained for each alloy. Fusion and solidification were performed in the water–cooled copper crucible of a CELES high frequency induction furnace. The obtained ingot, of several tens grams, were cut, embedded in a cold resin mixture and polished with SiC paper from 240 to 1,200 grit and finished using a textile disk enriched in 1µm diamond particles.

The metallographic characterization was done using a Scanning Electron Microscope (SEM: Philips, model XL30), mainly in the Back Scattered Electrons mode (BSE, 20kV), with acquisition of several micrographs (magnification×500 or ×1000) which were used both to illustrate microstructures and to estimate the carbides surface fractions (and of graphite when present) by image analysis (software Adobe Photoshop CS).

RESULTS AND DISCUSSION

Thermodynamic calculations

The calculated thermodynamic states of the binary

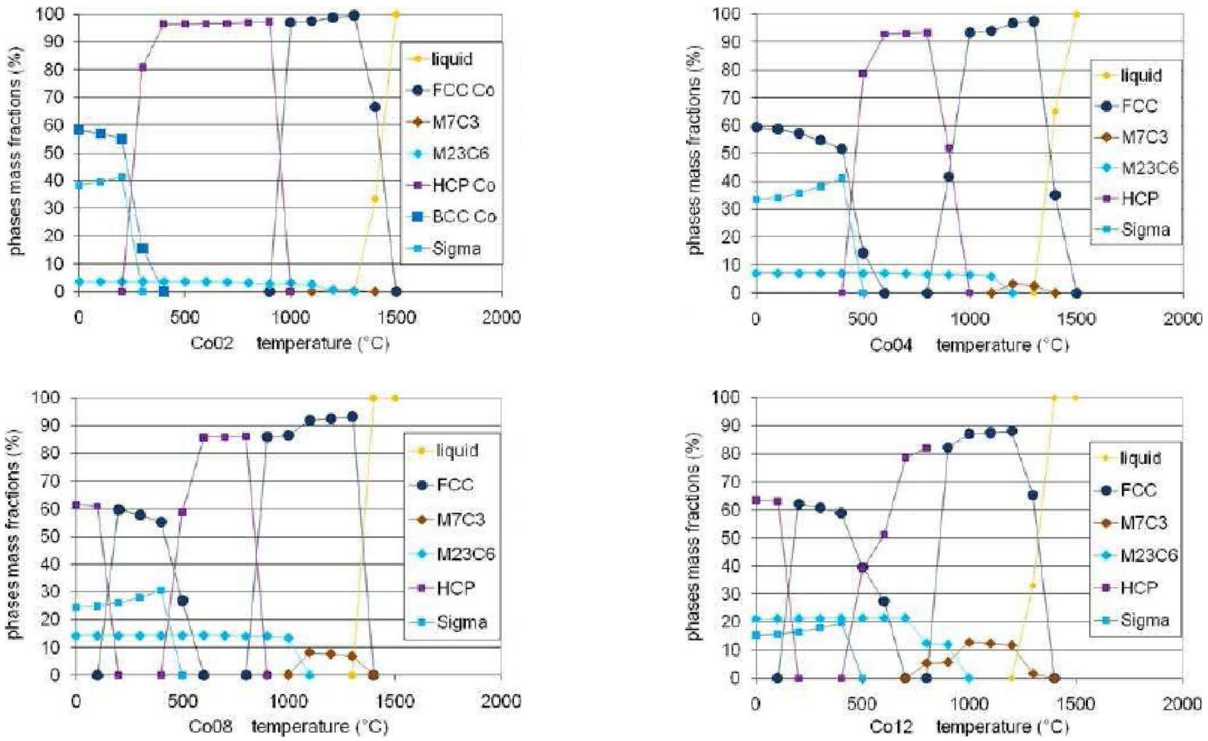

Figure 2 : Stable metallurgical states of the Co02 to Co12 alloys as calculated by Thermo-Calc; qualitative illustration of the microstructures development during the solidification progress

Co00 alloy at 1500°C and at lower temperatures, issued from Thermo-Calc are graphically represented in figure 1. This one can be interpreted, at least qualitatively, as the microstructure development of the alloy during the solidification stage, and during the solid state microstructure evolution during the first part of cooling (temperatures still high enough). Solidification logically leads to an unique phase, an austenitic Face Centred Cubic phase of cobalt containing chromium in solid solution. After total disappearance of the liquid phase, the FCC solid solution of cobalt remains alone until temperature reaches about 1000°C where the cubic network is replaced by a Hexagonal Compact Phase. According to Thermo-Calc this HCP solid solution of cobalt may disappear near 400°C, progressively replaced by two new phases, a Cr-impoverished Back Centred Cubic phase (cobalt containing less than 3%wt.Cr) and a CrCo sigma phase rich in chromium.

The addition of few carbon to the Co-30Cr base induces a significant decrease in solidus temperature (with as result an extended solidification temperature range) and the appearance of carbides (Cr_7C_3). The latter are the second solid phase to appear, after the FCC cobalt matrix. For low carbon contents (Figure 2) these Cr_7C_3 are rapidly (i.e. at very high temperatures) replaced by $Cr_{23}C_6$ carbides, but when the carbon content in the alloy increases, the temperature interval of existence of the Cr_7C_3 is more and more extended to the low temperatures, which delays the appearance of the $Cr_{23}C_6$ (about 1300°C for 0.2wt.%C → about 1000°C for 1.2wt.%C) while the weight percent of carbides progressively increases (e.g. more than 10 mass.% of Cr_7C_3 at high temperature and more than 20 mass.% for $Cr_{23}C_6$ at lower temperature for the Co12 alloy). This goes on for new increases in carbon content in the alloy (figure 3), with always a transition from $Cr_{23}C_6$ to Cr_7C_3 at a decreasing temperature, and for each of these carbides an increasing mass fraction. The two types of carbides, $Cr_{23}C_6$ (appeared near 700°C) and Cr_7C_3 (always appeared at high temperature) exist together over the [room temperature; about 700°C] range for the Co25 alloy, while there is no more $Cr_{23}C_6$ but Cr_3C_2 which replace (partly) the Cr_7C_3 carbides when the carbon content has become higher than about 3.0-3.5wt.% (Figure 4). A new carbide, cementite $(Co,Cr)_3C$ (almost Co_2CrC), also appears at high temperature, together with Cr_7C_3, for approximately the same carbon contents that lead

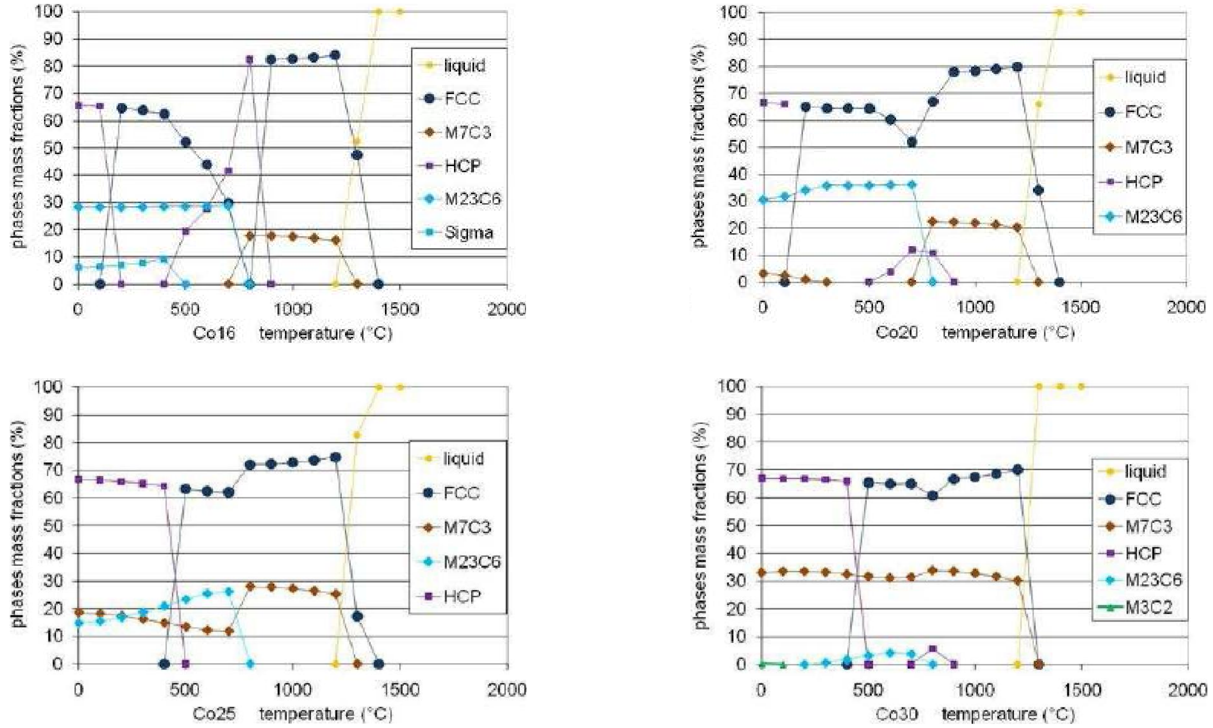

Figure 3 : Stable metallurgical states of the Co16 to Co30 alloys as calculated by Thermo-Calc; qualitative illustration of the microstructures development during the solidification progress

to Cr_3C_2 instead $Cr_{23}C_6$ at low temperature. For the maximal C content considered in this study, 5.0wt.% C, graphite also appears, but only under about 700°C while Cr_3C_2 is, for such a high carbon content, the unique carbide present over the (r.t. ; about 700°C) temperature range.

Concerning matrix, if the high temperature Cr-rich FCC solid solution of cobalt is replaced by the HCP one near 1000°C, and the latter would be replaced by a mix of Cr-impoverished BCC cobalt and sigma phase at about 250°C, the BCC form of cobalt does not appear anymore for carbon contents higher than 0.4wt.C. Thermodynamic calculations seem showing that it is FCC again which would appear together with the sigma phase at low temperature. For carbon contents high enough (2.0wt.%C and more), the two domains of FCC stability in temperature are joined together and FCC is the matrix network at high temperature (typically higher than 500°C) while HCP is the matrix network at low temperature (under 500°C). For the same high carbon contents, the maximal chromium content in FCC is 10wt.% Cr which decreases rapidly with temperature to almost zero, simultaneously with the change to HCP. The greatest part of chromium, then the whole chromium, is stored in the numerous carbides.

As-cast microstructures of the elaborated alloys

Figures 5, 6 and 7 display the as-cast microstructures respectively of the Co02 to Co12 alloys (low carbon contents and hypo-eutectic compositions), of the Co16 to Co30 (high carbon contents and hypo-eutectic compositions but near the eutectic one) and of the alloys with the highest carbon contents: Co35 (eutectic or slightly hyper eutectic) and Co40 to Co50 (hyper-eutectic). The hypo-eutectic character is revealed by the presence of dendrites of cobalt-based solid solution while carbides forming the eutectic compounds with the cobalt solid solution occupy the interdendritic spaces. The latter become more and more present (increasing surface fraction) and interconnected when the carbon content increases, until the latter reaches about 3.0-3.5wt.%, level at which the chemical composition is obviously eutectic. Indeed the microstructure has then become dendrites-free and only the {matrix + carbides} eutectic compound occupies the whole alloy structure. For higher carbon contents, supplementary coarse carbides are also present, with average size and total surface fraction which both increase with the carbon content. When the latter reaches 5 wt.% graphite appears in addition.

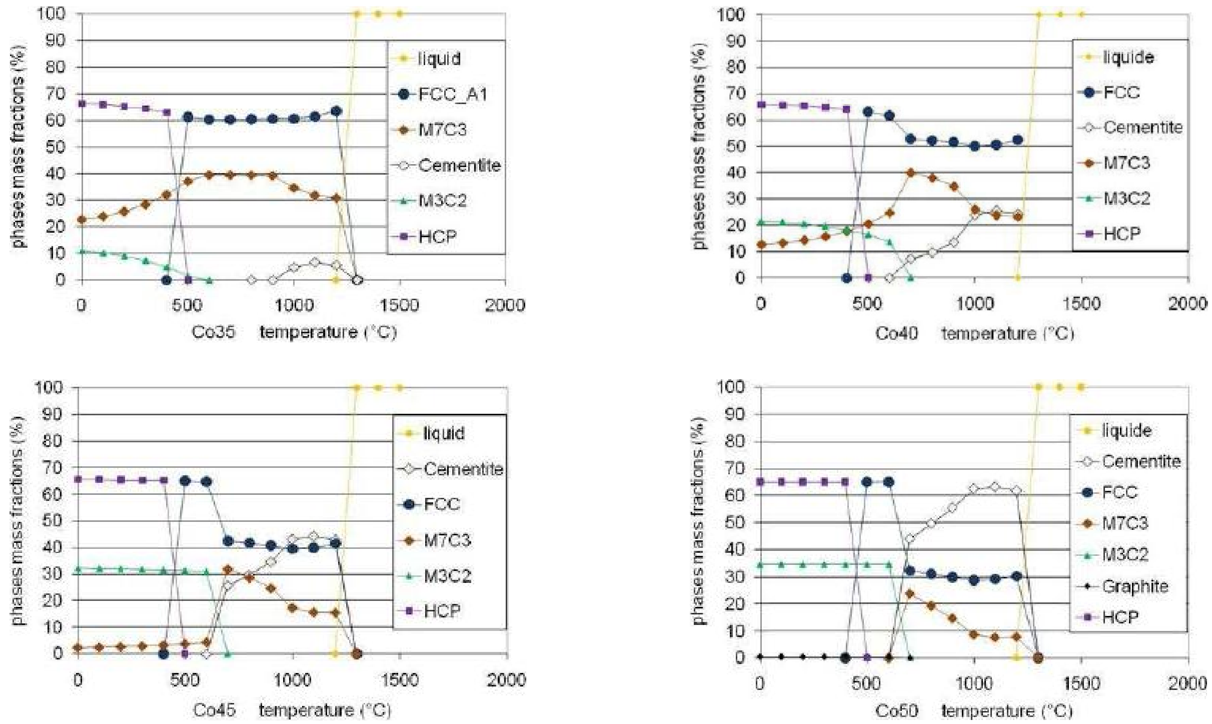

Figure 4 : Stable metallurgical states of the Co35 to Co50 alloys as calculated by Thermo-Calc; qualitative illustration of the microstructures development during the solidification progress

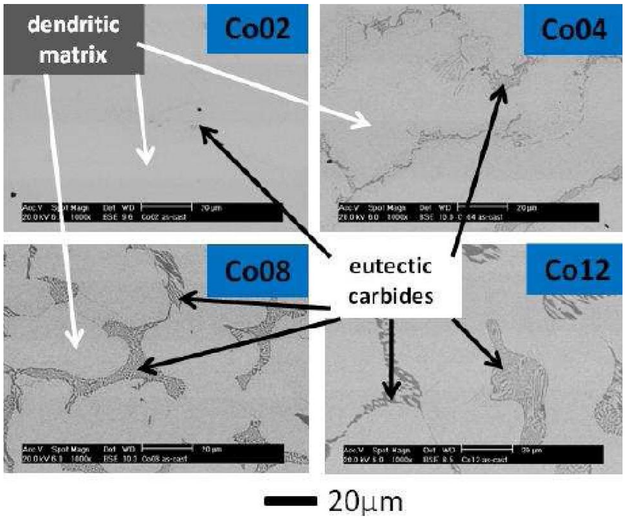

Figure 5 : As-cast microstructures of the low carbon hypo-eutectic alloys (Co02 to Co12)

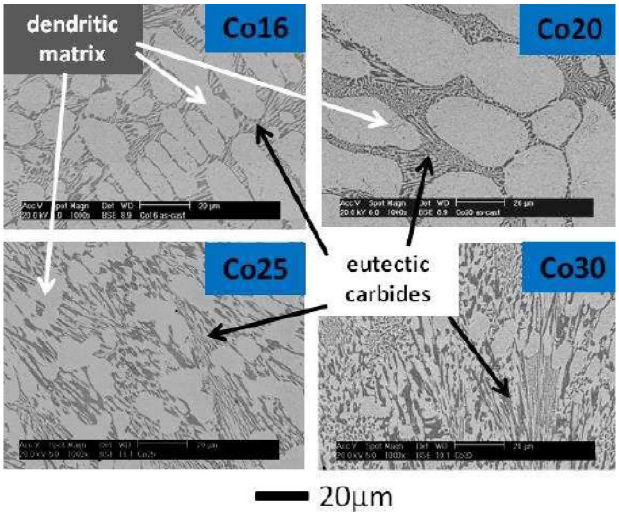

Figure 6 : As-cast microstructures of the high carbon hypo-eutectic alloys (Co16 to Co30)

These observations are qualitatively consistent with thermodynamic calculations which showed firstly that the FCC cobalt dendrites are the first solid phase to appear at the beginning of solidification for the lowest carbon contents in the studied range (which changes for carbon contents higher than 3wt.%), secondly that the carbide fraction logically increases with the carbon content, and thirdly graphite may appear (not at solidification but during solid state cooling) for the Co50 alloy. However there is no good agreement, quantitatively, between thermodynamic calculations results and the observed microstructures in the centres of the ingots analyzed by image analysis. The latter were performed, with Photoshop, generally for pictures taken at ×500 or ×1000, and the surface fractions, assumed to be close to the volume fractions, were converted in mass

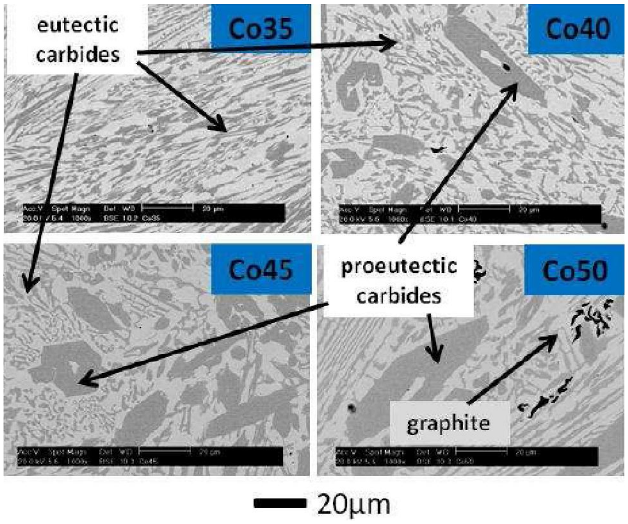

Figure 7 : As-cast microstructures of the very high carbon eutectic and hyper-eutectic alloys (Co35 to Co50)

fractions using 6.86 g/cm^3 (or 7.16 g/cm^3 if cementite can be present) for carbides (average of the densities of all types of carbides[7]: 6.97 ($M_{23}C_6$), 6.92 (M_7C_3), 6.68 (M_3C_2), 8.07 (cementite Co_3C) g/cm^3, 7.95 g/cm^3 for matrix and 2.25 g/cm^3 for graphite.

The comparisons between the as-cast phase fractions and the predicted ones which can be done are the following:

⇒ Co02 alloy: 0.29 surf.% of carbides, as is to say 0.25 mass.% (to compare to 0.3 – 3.6 mass.% calculated depending on temperature)

⇒ Co04 alloy: 3.7 surf.% of carbides, i.e. 3.2 mass.% (to compare to 2.5* –7.1** mass.% calculated)

⇒ Co08 alloy: 8.6 surf.% of carbides, i.e. 7.5 mass.% (to compare to 6.7 –14.3 mass.% calculated)

⇒ Co12 alloy: 8.8 surf.% of carbides, i.e. 7.6 mass.% (to compare to 11.8 –21.5 mass.% calculated)

⇒ Co16 alloy: 17.9 surf.% of carbides, i.e. 15.8 mass.% (to compare to 16.1 –28.7 mass.% calculated)

⇒ Co20 alloy: 13.0 surf.% of carbides, i.e. 11.4 mass.% (to compare to 20.2 –36.0 mass.% calculated)

⇒ Co25 alloy: 27.3 surf.% of carbides, i.e. 24.5 mass.% (to compare to 25.2 –37.9 mass.% calculated)

⇒ Co30 alloy: 31.6 surf.% of carbides, i.e. 28.5 mass.% (to compare to 30.0 –35.1 mass.% calculated)

⇒ Co35 alloy: 33.3 surf.% of carbides, i.e. 31.0 mass.% (to compare to 36.4 –39.6 mass.% calculated)

⇒ Co40 alloy: 38.6 surf.% of carbides, i.e. 36.1 mass.% (to compare to 47.5 –49.9 mass.% calculated)

⇒ Co45 alloy: 49.4 surf.% of carbides, i.e. 46.8 mass.% (to compare to 58.6 –60.6 mass.% calculated)

⇒ Co50 alloy: 47.6 surf.% of carbides and 1.68 surf.% graphite, i.e. 45.5 mass.% and 0.51 mass.% (to compare to 69.6 –71.2 mass.% and max 0.38 mass.% calculated). (* and ** for all alloys: * just after the solidification's end, ** at low/room temperature)

Comparisons between surface fraction measurements and thermodynamic calculations show that mass fractions deduced from surface fractions measured by image analysis are often a little, and sometimes significantly lower than predicted by Thermo-Calc. The greatest mismatches are mainly observed for the higher carbon contents, especially for Co12 (curiously poor in carbides with regards to its carbon content), Co20, and all the alloys between Co35 and Co50.

General commentaries

Similarly to the ternary nickel alloys[1] containing 30wt.%Cr and the same carbon quantities as here, a large variety of carbides fractions, as well as different morphologies were obtained in the cobalt-30wt.%Cr system. The limit in carbon content separating the hypo-eutectic and the hyper-eutectic alloys seems being higher than for the similar nickel alloys, since it is here about of 3wt.%C, as is to say significantly more than the 1.6-2wt.%C for the nickel-base family. This eutectic carbon content, of more than 1wt.% higher, leads to more alloys displaying a hypo-eutectic type of both solidification progress and thereafter microstructure (with dendrites of cobalt solid solution), and less hypereutectic alloys. A first consequence is that the elaboration by HF induction foundry led to less serious problems of lack of microstructure homogeneity: as illustrated by the micrographs given in figure 8 the external particular microstructures sometimes exist but are less deep than for the nickel alloys with the same carbon contents. A second consequence is that the appearance of graphite, which is possible for high carbon contents like for the

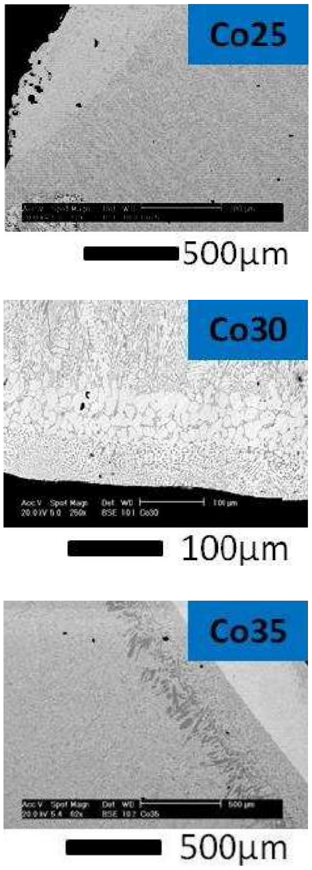

Figure 8 : Special microstructures sometimes observed in the outer parts of the ingots

nickel alloys, occurs for more carbon in the cobalt alloys (5 wt.% C) than for the nickel alloys (3.5-4 wt.% C). This leads to much more carbides in the cobalt-based alloys than in the nickel-based alloys as soon as the common carbon content in these two types of alloys is higher than 3.5 wt.%.

CONCLUSIONS

In 30wt.%Cr cobalt-based ternary alloys too, one can obtain very high carbides fractions by adding sufficiently carbon. Very high hardness values can be then expected in such cobalt alloys, notably with the possibility to obtain carbides fractions greater than for the nickel alloys thanks to a graphite appearance delayed to carbon contents much higher than in the nickel-30wt.%Cr system, and also to the intrinsic hardness of cobalt compared to the nickel one. Another advantage of this cobalt family alloy is, thanks to the high values of eutectic carbon content, a not too high proportion of coarse and acicular carbides which may favor crack propagation, phenomenon which particularly threatens very hard materials.

ACKNOWLEDGEMENTS

The authors thank Lionel Aranda and Thierry Schweitzer for their technical assistance.

REFERENCES

[1] P.Berthod, E.Souaillat, O.Hestin; Materials Science: An Indian Journal, submitted.

[2] D.A.Bridgeport, W.A.Brandtley, P.F.Herman; Journal of Prosthodontics, **2**, 144 **(1993)**.

[3] C.T.Sims, W.C.Hagel; 'The Superalloys', John Wiley & Sons, New York, **(1972)**.

[4] P.Berthod, J.L.Bernard, C.Liébaut; Patent WO99/16919.

[5] B.Roebuck, E.A.Almond; Int.Mater.Rev., **33**, 90 **(1988)**.

[6] A.Klimpel, L.A.Dobrzanski, A.Lisiecki, D.Janicki; J.Mater.Process.Tech., **164-165**, 1068 **(2005)**.

[7] G.V.Samsonov; 'Handbooks of High-Temperature Materials Properties Index', Plenum Press, New York, **2**, **(1964)**.

[8] P.Berthod; Materials Science and Technology, **25(5)**, 663 **(2009)**.

[9] Thermo-Calc Version N: 'Foundation for Computational Thermodynamics', Stockholm, Sweden, Copyright **(1993, 2000)**.

[10] A.Fernandez Guillermet; Int.J.Thermophys., **8**, 481 **(1987)**.

[11] J.O.Andersson; Int.J.Thermophys., **6**, 411 **(1985)**.

[12] P.Gustafson; Carbon, **24**, 169 **(1986)**.

[13] A.Fernandez Guillermet; Z.Metallkde, **78**, 700 **(1987)**.

[14] J.O.Andersson; Calphad, **11**, 271 **(1987)**.

[15] A.Fernandez Guillermet; Z.Metallkde., **79**, 317 **(1988)**.